A Long Distance Underwater Visible Light Communication System With Single Photon Avalanche Diode

Chao Wang
Hong-Yi Yu
Yi-Jun Zhu, *Member, IEEE*

A Long Distance Underwater Visible Light Communication System With Single Photon Avalanche Diode

Chao Wang, Hong-Yi Yu, and Yi-Jun Zhu, *Member, IEEE*

National Digital Switching System Engineering and Technological Research Center,
Zhengzhou, Henan Province 450000, China.

Abstract: Underwater visible light communication (UVLC) is of great interest to the military, industry, and the scientific community. In this paper, a long-distance UVLC system is designed, where the half power angle of light-emitting diode (LED) is narrowed to enhance the optical intensity at the transmitter, and a single photon avalanche diode (SPAD) is employed at the receiver to improve the detection sensitivity. A two-term exponential channel model of a long distance UVLC system with a SPAD receiver is established, and the channel parameters are obtained by Monte Carlo numerical simulation. Furthermore, the SPAD detection algorithm and the optimal detection threshold of the UVLC system are proposed. Simulation results show that the communication distance could be extended to 500 m in pure seawater.

Index Terms: Underwater visible light communication (UVLC), single photon avalanche diode (SPAD), channel model, Monte Carlo numerical simulation (MCNS).

1. Introduction

Due to the characteristics of green, ubiquitous, license free, and potential high bandwidth, visible light communication (VLC) has attracted increasing attention [1], [2]. Many experiments have been demonstrated for indoor high speed communications. In the meantime, outdoor VLC applications are utilized in several areas, such as lighthouses broadcastings, intelligent transportation systems and underwater communications [3]–[8]. Compared with laser diode used in the free space optical (FSO) communications, the light-emitting diode (LED) has much lower thermal resistance and, thus, can emit much higher optical power [4], [5].

Nowadays, underwater wireless information transmission is of great interest to the military, industry, and the scientific community. Although tremendous progress has been made in the field of underwater acoustic communication, its performance is limited by low bandwidth, high transmission losses, time varying multi-path propagation, high latency, and Doppler spread [6]. In an underwater environment, light propagation is wavelength sensitive with relative less attenuation in the blue/green wavelength range. Furthermore, the data rate of VLC is much higher than acoustic transmission in the water. Unlike radio frequency communication, VLC is not omnidirectional [7],
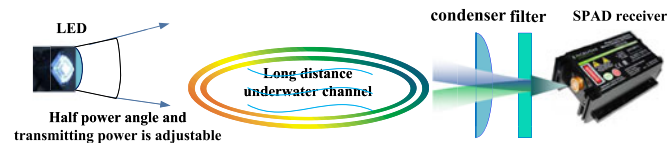
Fig. 1. Structure of a long distance UVLC system with SPAD.

[8], and it could benefit from a little interference. Therefore, VLC is a possible way to realize the future high-speed underwater communication network.

In general, to meet the normal illumination requirement in the indoor environment, VLC always works under relatively stronger optical intensity with the photoelectric detection devices, such as the photodiode (PD) and the avalanche photo diode (APD). However, the high detection threshold and high noise intensity come from trans-conductance amplifier (TIA) limit its practical application value for the long distance VLC system. When traditional detection devices and methods are used, the optical communication distance is less than 100 m in the pure sea seawater or the clear ocean due to the serious exponential attenuation [9]–[11].

Recent interests have been focused on applying single photon avalanche diodes (SPADs) to VLC. SPAD detectors do not require a TIA as it operates in the Geiger mode, and thus, the output signal is not distorted by thermal noise in the same way as in PDs/APDs [12]–[15]. For this reason, the exponential decay challenge of light intensity in the sea water will be relieved by the single photon detection [16], [17]. Consequently, it is possible that the communication distance of underwater visible light communication (UVLC) with a SPAD could be further extended.

To sum up, the contribution of this paper can be summarized as follows.

1) A long distance UVLC system is designed, where the half power angle of LED is narrowed to enhance the optical intensity at the transmitter, and a SPAD is used at the receiver to improve the detection sensitivity.
2) A two-term exponential channel model of the long distance UVLC system with SPAD receiver is established, and the channel parameters are obtained by Monte Carlo Numerical Simulation (MCNS).
3) The SPAD detection algorithm and the optimal detection threshold of the UVLC system are proposed.
4) A simulation system is constructed to examine the error performance of this long distance UVLC system, where the parameters are chosen in accordance with practical environment, practical devices and the existing experimental measurement data as far as possible. Simulation results show that the communication distance could be extended to 500 m in pure seawater.

2. System Model of UVLC With SPAD

The structure of the long distance UVLC system we designed is shown in Fig. 1. In order to extend the communication distance, two methods are adopted: 1) The half power angle of LED is narrowed by a lens to enhance the optical intensity at the transmitter, and 2) a SPAD is used at the receiver to improve detection sensitivity. The most difficult problem to analyze this system is that there is no long-distance underwater channel model for SPAD detection at present.

2.1. Lambert Model Analysis For LED Transmitter

For a generalized Lambertian radiant intensity light source, the relation between the radiation angle θ and the distribution of radiant intensity $\Psi_0(\theta)$ can be approximated as

$$\Psi_0(\theta) = \frac{(m_0 + 1)}{2\pi} \cos^{m_0}(\theta) \tag{1}$$

where $m_0 = -\ln 2/\ln(\cos\phi_0)$, and ϕ_0 denotes the half power angle of the LED. As the strict Lambertian source model, $\Psi_0(\theta)$ should meet the constraint of energy normalization condition [9], i.e., $2\pi \int_0^{\pi/2} \Psi_0(\theta)\sin(\theta)d\theta = 1$.

In this system, a certain lens, such as a reflective cup, is used to narrow the half power angle and to increase the light intensity of the commercial LED at the transmitter. As a common sense, the smaller the half power angle is, the stronger the intensity is, and thus, the further the communication transmits. We assume that the half power angle is narrowed as ϕ with $\phi < \phi_0$. Then, the distribution of radiant intensity $\Psi_1(\theta)$ can be approximated as

$$\Psi_1(\theta) = \frac{(m_1 + 1)}{2\pi}\cos^{m_1}(\theta) \tag{2}$$

where $m_1 = -\ln 2/\ln(\cos\phi_1)$. Thus, the intensity gain achieved by narrowing the half power angle is

$$G(\theta) = \frac{\Psi_1(\theta)}{\Psi_0(\theta)} = \frac{m_1 + 1}{m_0 + 1}\cos^{m_1 - m_0}(\theta). \tag{3}$$

Furthermore, in the center of the beam, i.e., $\theta \to 0$, the intensity gain can be approximated as

$$G_t = \frac{m_1 + 1}{m_0 + 1}. \tag{4}$$

2.2. Long Distance Underwater Channel Model For SPAD Receiver

Beer's law is commonly used to describe the underwater channel state in a short distance as

$$h(L) = h_c e^{-c(\lambda)L} \tag{5}$$

where $c(\lambda) = a(\lambda) + b(\lambda)$ denotes the cumulative attenuation coefficient. $a(\lambda)$ and $b(\lambda)$ are the absorption coefficient and scattering coefficient, respectively. λ is the wavelength of the light, L is the communication link distance, and h_c is a constant.

However, Beer's Law overlooks the indirect path. With the increase of distance, multiple scattering affects the main part of the channel loss and some photons may reach the receiver. Compared with Beer's Law model, a function of two exponentials could approximate the long distance underwater channel power loss more accurately. One exponential denotes the attenuation loss length less than the diffusion length and another one greater than the diffusion length. The diffusion length can be considered as the longest distance that a photon could travel theoretically [7], [9], which is defined as $\tau = c(\lambda)L$. Some research shows that underwater channel can be considered as non-dispersive if $\tau < 15$ and data rate is below than 50 Mbps [7], [8]. In fact, if we narrow the half power angel of LED and improve the power intensity, the underwater channel could be regarded as non-dispersive when the water quality is relative good. Consequently, the channel impulse response model versus communication distance is approximated by a delta function as

$$h(t, L) = (a_1 e^{-c_1 L} + a_2 e^{-c_2 L})\delta(t - L/v), \tag{6}$$

where $\delta(t - L/v)$ is the transmission delay. We assume that perfect symbol synchronization is performed at the receiver and inter-symbol-interference (ISI) could be neglected, then the channel model can be rewritten as

$$h(L) = a_1 e^{-c_1 L} + a_2 e^{-c_2 L}.$$

As far as we know, there is no universal theoretical model to describe the long distance optical communication with SPAD detection for practical underwater environment. Therefore, MCNS is the most widely used method to establish a channel impulse response versus communication distance [18]. The aim of MCNS for underwater optical environment is to trace the properties of a single mobile photon, including the direction, position, weight, distance, and others. The receiver determines whether the photon is received through a specific criterion. After independent repeated trials of a large number of photons launching and receiving, the MCNS results can be obtained.

Then, the parameters a_1, c_1, a_2, and c_2 of the two-term exponential function could be calculated by the least mean square fitting algorithm.

2.3. Signal Model and SPAD Receiver

Since intensity modulation with direct detection (IM/DD) has low-complexity and low-cost implementation, it is commonly used for VLC systems, which leads to the fact that the channel coefficients and the transmitting signals are nonnegative. The transmitted bit is chosen randomly, equally-likely, independently from a unipolar on-off keying (OOK) modulation constellation. When bit "1" is transmitted, the power of LED is $P_s = 2P_0$, and when bit "0" is transmitted, the power of LED is $P_s = 0$. Then, the average power of LED is $\bar{P} = P_0$, and the energy of LED can be defined as $E = P_0 T_b$, where T_b is the bit time duration, and $R_b = 1/T_b$ is the given bit data rate.

Since the output of SPAD is a photon count value, the received signal after optical direct detection can be given by

$$r(L) = P_s T_b G_t h(L) \eta \eta_o + N_{DCR} T_b \tag{7}$$

where $r(L)$ is the received photon number while $\eta = C_{PDE}/Ep$ with C_{PDE} is the photon detection efficiency, $Ep = hv/\lambda$ is the energy of a photon, v is the speed of light in water, and h is the Planck's constant. $\eta_o = \eta_t \eta_r \eta_l$ is the gain of the optics system, η_t and η_r are the transmittance of transmitter and receiver optics system, respectively, η_l is the gain of condenser. $\eta_l = n_{len}^2/\sin(\psi)^2$, where n_{len} denotes the refraction coefficient of optical glass lens, and ψ is the field-of-view angle of SPAD. In the MCNS simulation, we assume that a photon could be detected if it reaches the surface of the condenser. N_{DCR} is the dark count ratio of SPAD.

According to the analysis of [10], the downwelling solar background optical power on the detector is below -80 dBmW under the depth of hundreds of meters, even if the field of view angle is $90°$. Hence, we overlook underwater background optical radiations and consider that dark count is the exclusive noise.

The output photon number can be modeled as a poisson statistics distribution with the probability density function being expressed as

$$Pr(x, r) = \frac{r^x}{x!} e^{-r}, \tag{8}$$

where r is the mean of poisson distribution. For OOK modulation, the mean received photon numbers of SPAD are $N_1 = N_{r1} + N_{DCR} T_b$ and $N_0 = N_{DCR} T_b$ when the information of bit "1" and bit "0" are transmitted, respectively, where $N_{r1} = 2P_0 T_b G_t h(L) \eta \eta_o$. If the priori probabilities of bit "1" and bit "0" are equal, the optimum detection threshold of poisson distribution is the intersection point of curve $Pr(x, N_1)$ and $Pr(x, N_0)$:

$$\frac{N_1^x}{x!} e^{-N_1} = \frac{N_0^x}{x!} e^{-N_0} \tag{9}$$

and thus, we can obtain the optimum detection threshold as $x^* = \frac{N_{r1}}{\ln(1 + N_{r1}/N_0)}$. Then, we can make symbol judgements based on the receiving photon number and the optimum detection threshold.

3. Simulation and Discussion

In this section, we will obtain the channel model for the long distance UVLC by MCNS. Then we will examine the error performance of UVLC under different LED powers, different half power angles, and different communication distance. To make the simulation as persuasive as possible, the parameters used in the simulation are chosen in accordance with the practical environment and practical devices.

In the simulation, we consider two types of underwater environments: pure seawater and clean ocean. The corresponding attenuation coefficients that come from actual measurement [18] are listed in Table I.

TABLE I

Attenuation Coefficients for Different Water Types

Water Type	$a(\lambda)$ (m^{-1})	$b(\lambda)$ (m^{-1})	$c(\lambda)$ (m^{-1})
Pure Seawater	0.053	0.003	0.056
Clean Ocean	0.069	0.08	0.15

TABLE II

Parameters of SPAD and the Optics System

Wavelength of light (λ)	532 nm
The PDE of the SPAD (C_{PDE})	0.35
The DCR of the SPAD (N_{DCR})	50
Dead time of the SPAD	20 ns
Field of view angle of the receiver (ψ)	10°, 30°
Detector aperture diameter of the receiver	0.044 m
Transmittance of the receiver optics system (η_r)	0.7
Transmittance of the transmitter optics system (η_t)	0.8
Refraction coefficient of optical lens (n_{len})	1.5
Half power angle of the transmitter (ϕ)	5°, 10°

We consider the blue/green light band of 430 $\sim$ 550 nm in the simulation environment. A narrow optical filter with a central wavelength of 532 nm is used at the receiver. Furthermore, we assume that the under water environment is an ideal isotropic, homogeneous medium without flowing, and we can treat the UVLC channel as a linear time-invariant system. Similar to the experiment in [7], [11], we assume that transmitter and receiver planes are aligned to the light beam. Therefore, the receiver could detect the light beam focus effectively and the beam deflection can be overlooked.

For the purpose of acquiring accurate and realistic results, we choose the system parameters, such as beam width (0.00075 m), beam divergence (0.001 m), water type, and aperture size, to be the same as Petzold used in the experiment in San Diego Harbor [7], [11]. The parameters of the SPAD (Excelitas Technologies Company, SPCM-AQRH-15-FC) and the optics system are listed in Table II. The operating temperature of the SPAD ranges from 5° to 30°, which covers the practical underwater temperature range.

3.1. Channel Simulation for Long Distance UVLC

In the previous channel simulation for UVLC, such as Akhoundi's simulation model, is based on relative closer range and treats the light source as an equivalent spherical model. However, in this system, the channel gain is enhanced through a narrower beam. Furthermore, the simulations should be simulated for an open water circumstance rather than a sealed water tank. The channel simulation we performed includes two steps as follows:

Step 1: MCNS of UVLC channels for different conditions. At first, we simulate the propagation process of massive photons, and record the detected photons by MCNS at the receiver for a given distance. The value of photon weight threshold at the receiver is set as 10^{-6}, which corresponds to the detection sensitivity of SPAD. In order to reduce the influence of dark count, we should ensure

TABLE III

Channel Parameters for Different Water Types and Polar Angles

Water Type (half power angle)	a_1	c_1	a_2	c_2
Pure Seawater (5°)	0.1999999	0.0657156	0.0046431	0.2633946
Pure Seawater (10°)	0.0859942	0.0702351	0.0112750	0.2998076
Clean Ocean (5°)	0.0999882	0.1518284	0.1588808	0.4936873
Clean Ocean (10°)	0.0519135	0.1592843	0.1189797	0.5071980
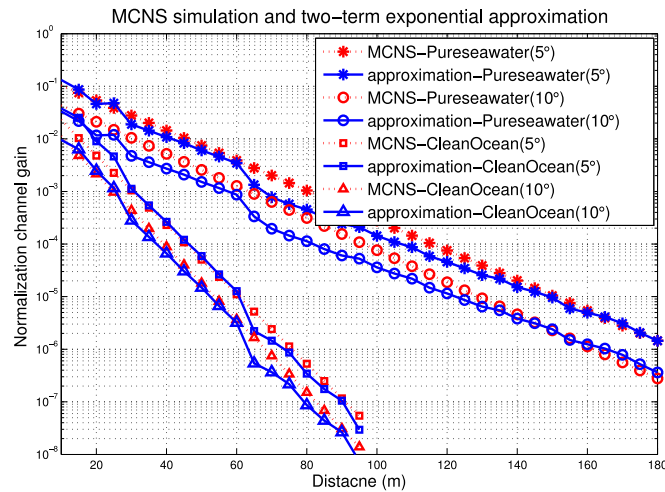
Fig. 2. Normalized channel gain comparisons of MCNS and tow-term exponential function approximation under different different water types and different half power angles.

that there are at least 20 detected photons at the receiver in each bit duration. In our simulations, there are at least 10^9 launching photons in each bit duration. Then, we can get a curve about channel's intensity versus communication distance by normalizing the statistics of the total transmit energy. Finally, we can obtain a series impulse response curves of UVLC under different conditions, including different water types and different half power angles.

Step 2: Two-term exponential approximations of UVLC channels. Then, we use two-term exponential function to fit the MCNS results by deploying the least mean square error algorithm. The fitting range of four parameters (a_1, c_1, a_2, c_2) are among (0:1), and the parameters we obtained are listed in Table III.

The normalized channel gain comparisons of MCNS and two-term exponential function approximation under different conditions are shown in Fig. 2. It can be concluded that when the communication distance is longer than 180 m, the approximate error is small than 10^{-5}. Hence, we will use the two-term exponential function as the channel model in the next simulation.

3.2. Error Performance Simulations of Long Distance UVLC

In this subsection, we examine the error performance of long distance UVLC with SPAD under different system configurations. The average power of LED is $\bar{P} = 1$ W, 10 W, and 100 W, and its half power angle is $\phi = 5°$, 10°. The field of view angle of the SPAD is $\psi = 10°$, or 30°. The data rate is $R_b = 1$ Mbps, 10 Mbps, or 50 Mbps. The maximum data rate of 50 Mbps corresponds to

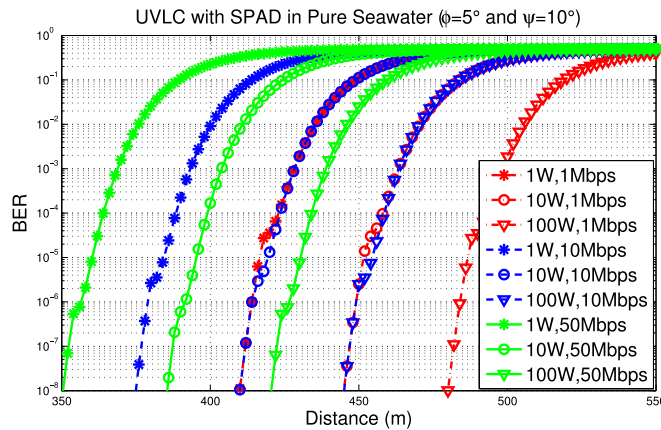Fig. 3. BER performance of UVLC in pure seawater for different LED powers and rates when $\phi = 5°$, $\psi = 10°$.
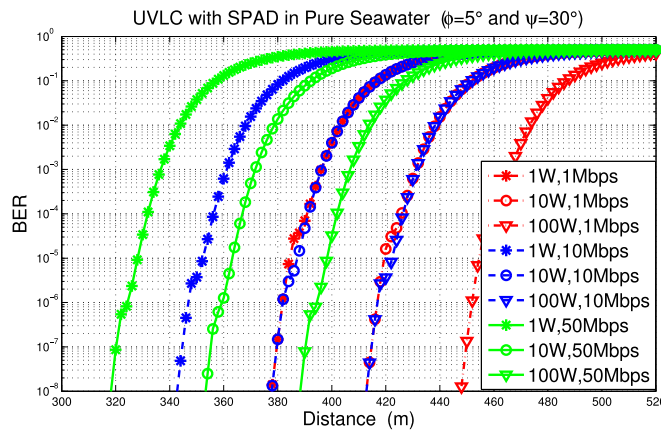

Fig. 4. BER performance of UVLC in pure seawater for different LED powers and rates when $\phi = 5°$, $\psi = 30°$.

the conclusion of the bit duration approximately equals the dead time [15]. Pure seawater and clear ocean environments are considered, and the channel model are adopted using the two-term exponential functions obtained in the above subsection.

We omit the underwater background optical radiations and consider that dark count is the exclusive noise. When bit "1" is transmitted, the power of LED is $P_s = 2P_0$, and the photon number is $2P_0 T_b / E_p$; while bit "0" is transmitted, the power of LED is $P_s = 0$. For each bit duration, we record the output photon number of SPAD and make a judgement on whether the number is bigger than the threshold or not. Then, BERs can be achieved for different distances.

When $\phi = 5°$, Figs. 3 and 4 show the BER performance of ULVC in pure seawater with $\psi = 10°$ and $30°$, respectively. We can observe that when $\bar{P} = 100$ W, $R_b = 1$ Mbps, $\psi = 10°$, and the communication distance is 500 m, the corresponding BER is about 2×10^{-3}, which is much closer to the forward-error-correction (FEC) limit of 3.8×10^{-3} and some FEC codes can provide reliable communication with an overhead of approximately 7% [19]. Therefore, we can obtain that the furthest distance could be reach nearly 500 m for a UVLC system with SPAD. Meanwhile, we can also observe that underwater channel can support high-speed VLC. A 50 Mbps UVLC system can work at a distance of 440 meters when $\bar{P} = 100$ W, $\psi = 10°$, and at a distance of 335 m when $\bar{P} = 1$ W, $\psi = 30°$.

When $\phi = 10°$, Figs. 5 and 6 show the BER performance of ULVC in pure seawater with $\psi = 10°$ and $30°$, respectively. Since the attenuation comes from photon absorption and scattering would be
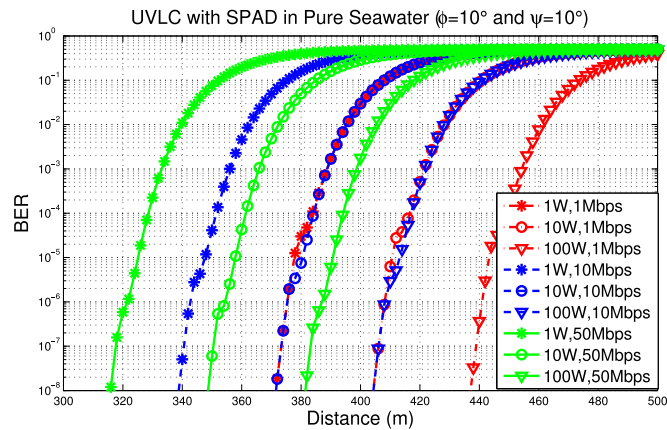
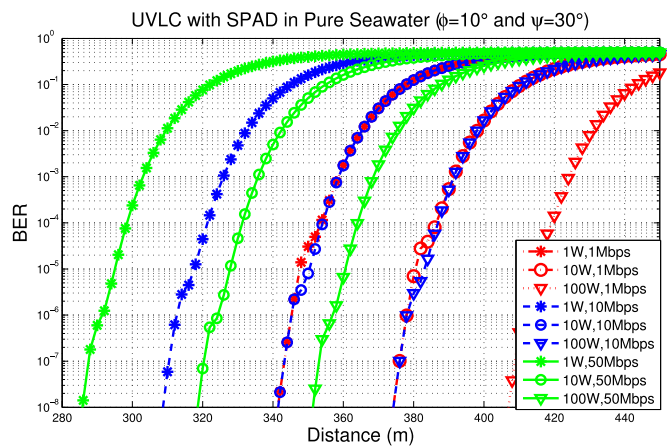Fig. 5. BER performance of UVLC in pure seawater for different LED powers and rates when $\phi = 10°$, $\psi = 10°$.

Fig. 6. BER performance of UVLC in pure seawater for different LED powers and rates when $\phi = 10°$, $\psi = 30°$.

more serious when the half power angle increases. The communication distance becomes shorter. Coincidentally, the two curves are almost overlapped when $\bar{P} = 1$ W, $R_b = 1$ Mbps and $\bar{P} = 10$ W, $R_b = 10$ Mbps; Furthermore, the two curves are also overlapped when $\bar{P} = 10$ W, $R_b = 1$ Mbps and $\bar{P} = 100$ W, $R_b = 10$ Mbps. Since the transmitting energy of each bit is $E = 2P_0 T_b$, the receiving energy between $\bar{P} = 1$ W, $R_b = 1$ Mbps and $\bar{P} = 10$ W, $R_b = 10$ Mbps is the same. Therefore, in the simulations, the curves are almost overlapped to some extent. A similar conclusion is suited for $\bar{P} = 10$ W, $R_b = 1$ Mbps and $\bar{P} = 100$ W, $R_b = 10$ Mbps.

Similar simulation results for clear ocean environment are shown in Figs. 7, 8, 9 and 10. Comparing with the pure seawater environment, we can observe that the communication distance reduces because the clear ocean suffers from a relative serious attenuation. However, the effective communication distance is still about 143 m with $\phi = 5°$ and 130 m with $\phi = 10°$ when $R_b = 50$ Mbps, $\bar{P} = 1$ W.

3.3. Performance Comparison for APD and SPAD

In this sub-section, we will compare the performance of UVLC systems with the SPAD receiver and the APD receiver. In order to compare with the data rate, communication distance achieved with APD in [18], we set the parameters of the SPAD receiver and the APD receiver as identically as possible. The dead time of SPAD is 10ns and the maximum data rate is 100 Mbps. The power of LED is set as 1 W. The half power angle of both receivers is narrowed as 5° or 10°. The field of
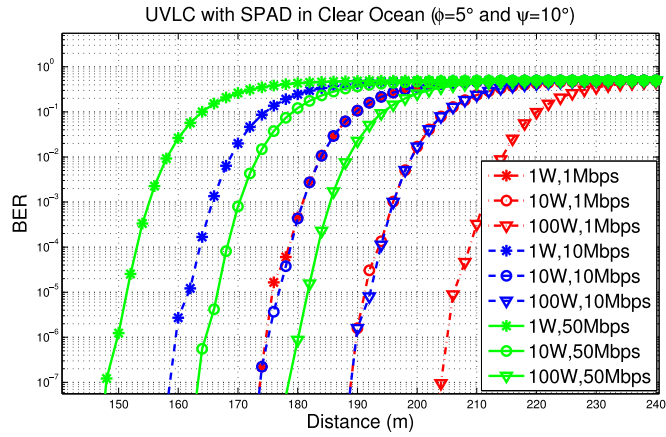
Fig. 7. BER performance of UVLC in clear ocean for different LED powers and rates when $\phi = 5°$, $\psi = 10°$.
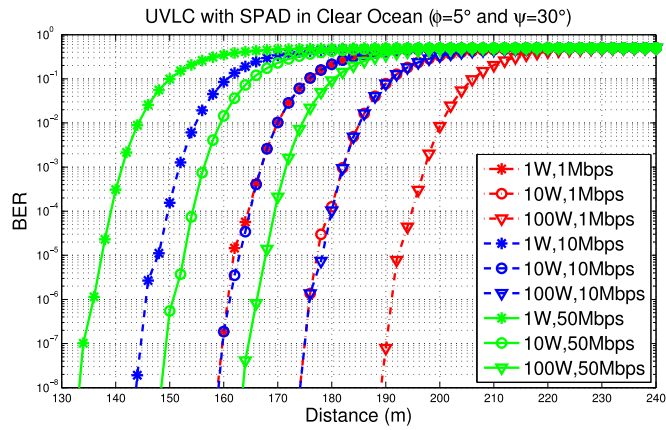

Fig. 8. BER performance of UVLC in clear ocean for different LED powers and rates when $\phi = 5°$, $\psi = 30°$.
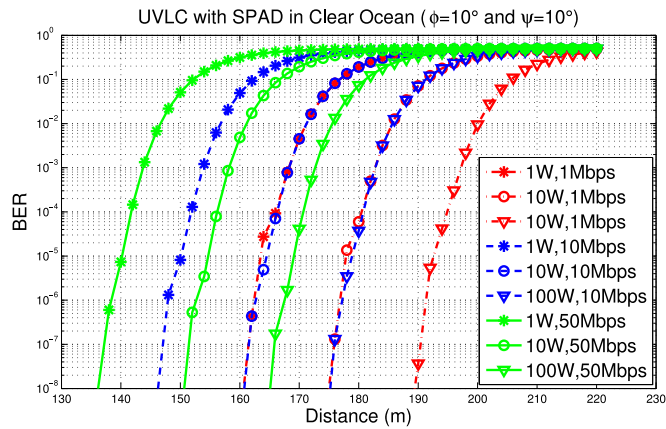

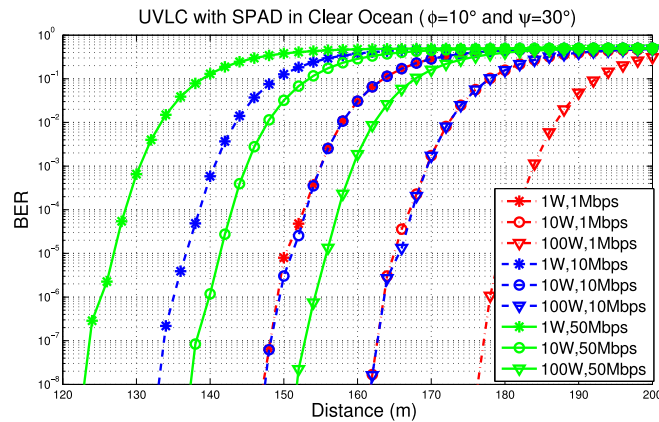Fig. 9. BER performance of UVLC in clear ocean for different LED powers and rates when $\phi = 10°$, $\psi = 10°$.

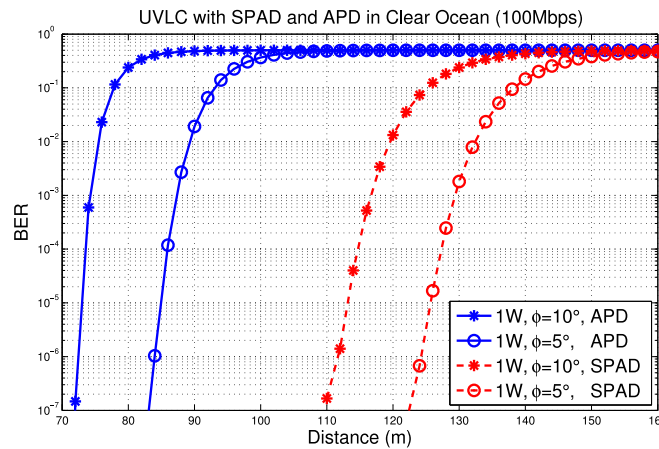Fig. 10. BER performance of UVLC in clear ocean for different LED powers and rates when $\phi = 10°$, $\psi = 30°$.

Fig. 11. Performance comparison for APD and SPAD receiver.

view angle of both receivers is $\psi = 30°$. Fig. 11 shows the simulation results for BER performance comparison between SPAD receiver and APD receiver. We can observe that for the SPAD receiver, the communication distance is about 112 m for the target BER of 10^{-6} when $\bar{P} = 1$ W, $\phi = 10°$ and $R_b = 100$ Mbps in clear ocean. However, the corresponding distance for APD receiver is about 73 m in [18]. When $\theta = 5°$, the communication distances of the SPAD and APD receivers are 125 m and 83 m, respectively. It can be concluded that the SPAD receiver can extend the transmission distance effectively for UVLC.

4. Conclusion

In this paper, a long-distance UVLC system has been designed, where the half power angle of LED is narrowed to enhance the optical intensity at the transmitter, and a SPAD is used at the receiver to improve the detection sensitivity. Additionally, the channel model of the long distance UVLC system with SPAD receiver is established by using MCNS. Simulation results show that the communication distance could be extended to 500 m in pure seawater. In the near future, we will perform some practical experimental measurements on the long-distance UVLC system.

References

[1] T. Komine and M. Nakagawa, "Fundamental analysis for visible-light communication system using LED lights," *IEEE Trans. Consum. Electron.*, vol. 50, no. 1, pp. 100–107, Feb. 2004.

[2] A. Jovicic, J. Li, and T. Richardson, "Visible light communication: Opportunities, challenges and the path to market," *IEEE Commun. Mag.*, vol. 51, no. 12, pp. 26–32, Dec. 2013.

[3] N. Lourenço, D. Terra, N. Kumar, L. N. Alves, and R. L. Aguiar, "Visible light communication system for outdoor applications," in *Proc. 8th Int. Symp. Commun. Syst., Netw. Digit. Signal Process.*, 2012, pp. 1–6.

[4] Y. G Wang, X. X Huang, L. Tao, and N. Chi, "1.8-Gb/s WDM visible light communication over 50-meter outdoor free space transmission employing CAP modulation and receiver diversity technology," in *Proc. Opt. Fiber Commun. Conf. Exhib.*, 2015, pp. 1–4.

[5] M. L Zhang, P. Zhao, and Y. J Jia , "A 5.7 Km visible light communications experiment demonstration," in *Proc. 7th Int. Conf. Ubiquitous Future Netw.*, 2015, pp. 1–3.

[6] H. Kaushal and G. Kaddoum, "Underwater optical wireless communication," *IEEE Access*, vol. 4, no. 4, pp. 1518–1547, Apr. 2014.

[7] F. Akhoundi, J. A. Salehi, and A. Tashakori, "Cellular underwater wireless optical CDMA network: Performance analysis and implementation concepts," *IEEE Trans. Commun.*, vol. 63, no. 3, pp. 882–891, Mar. 2015.

[8] S. J. Tang, Y. H. Dong, and X. D. Zhang, "Impulse response modeling for underwater wireless optical communication links," *IEEE Trans. Commun.*, vol. 62, no. 1, pp. 882–891, Jan. 2014.

[9] W. C. Cox, "Simulation, modeling, and design of underwater optical communication systems," Ph.D. dissertation, Elect. Eng. Dept., North Carolina State University, Raleigh, NC, USA, 2012.

[10] J. W. Giles and I. N. Bankman, "Underwater optical communications systems, Part 2: Basic design considerations," in *Proc. IEEE Mil. Commun. Conf.*, 2005, pp. 1700–1705.

[11] T. Petzold, "Volume scattering furctions for selected ocean waters," *Scripps Institution of Oceanography Visibility Laboratory*, San Diego, CA, USA, Oct. 1972.

[12] Y. C. Li, M. Safari, R. Henderson, and H. Haas, "Optical OFDM with single-photon avalanche diode," *IEEE Photon. Technol. Lett.*, vol. 27, no. 9, pp. 943–946, May 2015.

[13] Y. C. Li, S. Videv, M. Abdallah, K. Qaraqe, M. Uysal, and H. Haas, "Single photon avalanche diode (SPAD) VLC system and application to downhole monitoring," in *Proc. IEEE Glob. Commun. Conf.*, May 2014, pp. 2108–2113.

[14] D. Chitnis *et al.*, "A 200 Mb/s VLC demonstration with a SPAD based receiver," in *Proc. Summer Topicals Meeting Ser.*, Jul. 2015, pp. 226–227.

[15] D. Chitnis and S. Collins, "A SPAD-based photon detecting system for optical communications," *J. Lightw. Technol.*, vol. 32, no. 10, pp. 2028–2034, May 2014.

[16] P. A. Hiskett and R. A. Lamb, "Underwater optical communications with a single photon-counting system," in *Proc. Soc. Photo-Opt. Instrum. Eng.*, vol. 9114, 91140, pp. 1–15, May 2014.

[17] P. A. Hiskett, R. A. Struthers, R. Tatton, and R. Lamb, "A photon-counting optical communication system for underwater data transfer," in *Proc. Soc. Photo-Opt. Instrum. Eng.*, vol. 8542, 854214, pp. 1–16, Nov. 2012.

[18] C. Gabriel, M. A. Khalighi, S. Bourennane, P. Lon, and V. Rigaud, "Monte-Carlo-based channel characterization for underwater optical communication systems," *J. Opt. Commun. Netw.*, vol. 5, no. 1, pp. 1–11, Jan. 2013.

[19] ITU-T, "Forward error correction for high bit-rate DWDM submarine systems," (*ITU*, 2004), [Online]. Available: http://www.itu.int/rec/T-REC-G.975.1-200402-I/en.